

Temperature dependence of open-circuit voltage and recombination processes in polymer–fullerene based solar cells

Anil K. Thakur^a, Guillaume Wantz^a, Germà Garcia-Belmonte^b, Juan Bisquert^b, Lionel Hirsch^{a,*}

^a University of Bordeaux, IMS Laboratory, CNRS UMR 5218, ENSCBP, 16 Av. PeyBerland 33607, Pessac Cedex, France

^b Departament de Física, Photovoltaic and Optoelectronic Devices Group, Universitat Jaume I, ES-12071 Castelló, Spain

ARTICLE INFO

Article history:

Received 4 February 2011

Received in revised form

24 February 2011

Accepted 6 March 2011

Keywords:

Organic solar cells

Bulk heterojunction

Charge carrier lifetime

ABSTRACT

In this article, we have studied the temperature and illumination dependence of open-circuit voltage (V_{OC}) in polymer–fullerene based solar cells. It has been observed that V_{OC} at higher illumination intensities gets converged at 0 K which gives information about maximum achievable V_{OC} in a particular donor–acceptor blend. Besides this, recombination processes have been studied by transient open-circuit voltage decay (TOCVD) and the transition between recombination regimes has been observed for the first time. At low V_{OC} carrier lifetime exhibits a constant value around 500 μs, which is interpreted in terms of a monomolecular recombination regime. At higher V_{OC} carrier lifetime decreases as derived from a bimolecular relaxation law. The method allows estimating the recombination coefficient, which results in $2 \times 10^{-13} \text{ cm}^3 \text{ s}^{-1}$. The results have been explained by considering Gaussian density-of-states (DOS) for highest-occupied molecular orbital (HOMO) and lowest-unoccupied molecular orbital (LUMO).

© 2011 Elsevier B.V. All rights reserved.

1. Introduction

Well known thermodynamic arguments proposed by Shockley and Queisser [1] are based on considering radiative recombination as the only loss process which puts a fundamental upper limit on the energy conversion of solar cells. The highest reported efficiency of polymer–fullerene solar cells [2] is far below the radiative limit of Shockley and Queisser [1]. The internal quantum efficiency polymer–fullerene photovoltaic systems have reached $\approx 100\%$ [2]; this implies that energy conversion efficiency must be mainly limited by the open-circuit voltage (V_{OC}). The V_{OC} is found to scale with $E_g = \{E_{LUMO(A)} - E_{HOMO(D)}\}$ of the blend, i.e. the difference between the highest-occupied molecular orbital (HOMO) of electron donor material and the lowest-unoccupied molecular orbital (LUMO) of the electron acceptor material [3] which is equivalent to ionization potential and electron affinity of respective materials. Therefore, a significant energy loss arises from the difference of electron affinity and ionization potential of the electron acceptor and donor materials, respectively. The exciton binding energy in organic semiconductor can be as high as $\approx 1.5 \text{ eV}$ [4]; therefore a blend of two materials with different electron affinities and ionization potentials has to be used for exciton dissociation and generation of free charge carriers at interfaces [5] in polymer–fullerene solar cells.

Although the recombination losses mainly take place at the donor/acceptor interface, the role of energetic disorder cannot be ignored, which is inherent to organic layers. The recombination processes and the maximum attainable V_{OC} of polymer–fullerene solar cells are still under investigation. It is a thumb rule that V_{OC} is related to $E_g = \{E_{LUMO(A)} - E_{HOMO(D)}\}$ but it depends upon a number of parameters, e.g. illumination intensity, temperature, exciton generation rate, mobility of charge carrier, charge carrier lifetime and recombination rates. It is necessary to study recombination processes for understanding of origin and nature of V_{OC} .

In the present paper, we have studied the temperature and intensity dependent characteristics of poly (3-hexylthiophene) (P3HT) and phenyl-C₆₁-butyric acid methyl esters (PCBM) based solar cells. The most exciting trend is that all the curves at different intensities of illumination (higher than threshold illumination) are converging at 0 K and it is also the maximum attainable V_{OC} for a donor–acceptor combination. The charge carrier lifetime has been measured by transient open-circuit voltage decay (TOCVD) method. The transition between recombination regimes has been observed for the first time. The observed results have been explained by considering Gaussian DOS for highest-occupied molecular orbital (HOMO) and lowest-unoccupied molecular orbital (LUMO).

2. Experimental

Devices based on P3HT (Plextronic, 99.5%) and PCBM (Aldrich, 99.5%) have been fabricated from their blended solution

* Corresponding author.

E-mail address: lionel.hirsch@ims-bordeaux.fr (L. Hirsch).

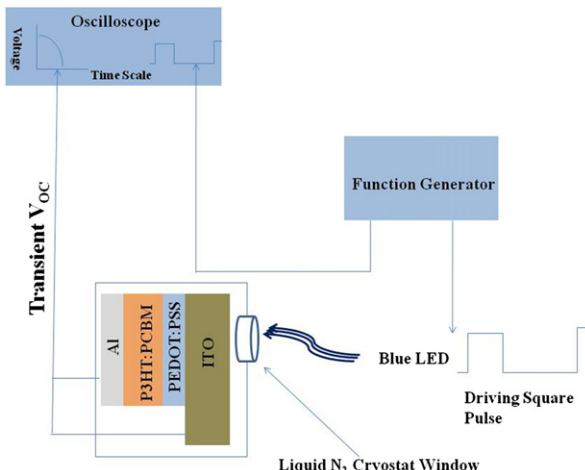


Fig. 1. Experimental set-up for transient open-circuit voltage decay (TOCVD).

(1:1, 20 mg/ml) in chloro-benzene by spin-coating on a PEDOT:PSS (≈ 50 nm) coated ITO glass substrate. To change the preparatory conditions, samples are unannealed or annealed before (pre-annealed, 140 °C for 10 min) or after (post-annealed, 160 °C for 10 min) the deposition of top aluminum electrodes. Efficient PV cells are fabricated after the deposition of aluminum (Al) anode (100 nm); the devices are post-annealed at 160 °C for 10 min. The efficiency of this device has been found to be 3.23% ($V_{OC}=0.58$ V, $J_{SC}=8.28$ mA/cm², $V_{max}=0.41$ V, $J_{max}=7.41$ mA/cm² and Fill factor = 63.4%) under illumination of (100 mW/cm²) white light from AM 1.5G solar simulator at 300 K. The area of the device is 8.5 mm² and thickness of active layer is ≈ 100 nm. Temperature dependent measurements are carried-out inside a liquid nitrogen cryostat. The sample has been affixed on sample holder inside cryostat with silver paste that also acts as heat sink. High power blue LED ($\lambda_{max}=480$ nm) has been used as light source and its illumination level has been normalized due to experimental constraints. The output power of LED linearly varies with driving current. For six different driving currents [10–700 mA], absolute output powers of LED as measured with a *Labsphere 6"* calibrated integrated sphere are 4.7, 32, 63, 122, 215 and 315 mW for Light 1, Light 2, Light 3, Light 4, Light 5 and Light 6, respectively. During the experiment, the geometry of the set-up is carefully kept unchanged in order to preserve the proportionality of the illumination intensity with the LED output. The schematic diagram for open-circuit voltage decay has been shown in Fig. 1.

3. Results and discussions

Temperature dependence of V_{OC} has been reported earlier but different trends have been observed [6–11]. We found that leakage current densities (J_L) play a crucial role in the V_{OC} versus temperature characteristics. Here, the temperature dependence of open-circuit voltage has been studied in P3HT:PCBM based solar cells. The devices have been fabricated in different preparation conditions and temperature dependence of V_{OC} has been observed to be linked with temperature dependence of leakage current densities. At V_{OC} , the sum of generated photo-current density (J_{ph}), recombination current density (J_R) and J_L should be equal to zero. Thus, J_R must be much greater than J_L to observe material instead of device properties. Therefore, a minimum leakage current density is prerequisite requirement for high V_{OC} . In other words, if $J_R \gg J_L$, generation rate (G) equals recombination rate (R) because of negligible shunt current. As shown in Fig. 2, V_{OC} versus

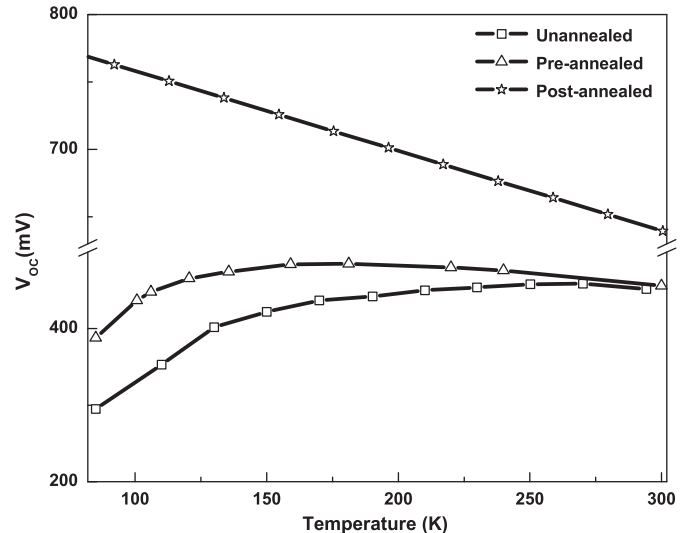


Fig. 2. Temperature dependence of open-circuit voltage in devices with different preparatory conditions under 315 mW illumination of blue LED ($\lambda_{max}=480$ nm). The leakage currents (J_L) at -1 V and 300 K for unannealed, pre-annealed and post-annealed devices are 0.51, 0.31 and 0.06 mA/cm², respectively.

temperature curves for pre-annealed (before anode deposition) and unannealed devices show minimum V_{OC} at lowest temperature (85 K) whereas post-annealed devices show highest V_{OC} . Temperature dependent V_{OC} is linear for P3HT:PCBM based solar cells with power conversion efficiency $> 3\%$ and with low J_L values. If $J_L \approx J_R$, shunt current cannot be neglected and V_{OC} is then reduced. So, only the annealed PV cells at 160 °C after deposition of Al electrode have been chosen for further study.

In Fig. 3(a) and (b), the J - V characteristics of solar cells have been shown at 300 and 85 K, respectively. The V_{OC} is changed as the intensity of illumination is changed as reported [12,13]. It is also evident that V_{OC} depends on both temperature and illumination intensities. V_{OC} increases as temperature is reduced or illumination is increased. It can also be seen that photocurrents are about 2 orders of magnitude higher than dark currents (even at -1 V and at the lowest illumination intensity). Moreover, reduction of dark current at low T results from the reduction of both charge carriers mobility and injection.

The question arises, why does V_{OC} vary either with temperature or illumination intensity? We first check if the band gap of materials is varying with temperature (T). Temperature dependent incident photon to current efficiency (IPCE) study has then been carried-out. Spectra are presented in Fig. 3(c) which show that absorption of the blend remains constant between 80 and 300 K. Therefore, we may rule out the variation in band gap of the blend with temperature. It can also be clearly seen from Fig. 3(d) that J_{SC} is constant as temperature is reduced to a certain critical temperature (T_C) for particular intensities. This has been shown by a red dotted line in Fig. 3(d). Above T_C , it demonstrates that the generation rate is constant. On the further reduction of temperature below this T_C , the J_{SC} is reducing which implies that mobility is reduced below T_C , i.e. transit time is higher than the lifetime of charge carriers; therefore it recombinates before reaching electrodes. With this methodology, it is only possible to demonstrate that G does not vary with T above T_C ; however, we guess that the diminution of J_{SC} below T_C originates only from the reduction of charge carrier mobility and not due to a decrease of G .

Under illumination, V_{OC} is related to the splitting of quasi Fermi levels, which depend on the charge carrier densities in the LUMO and HOMO density-of-states [14]. In a steady state, G and R are in equilibrium, which set the charge carrier densities [15,16].

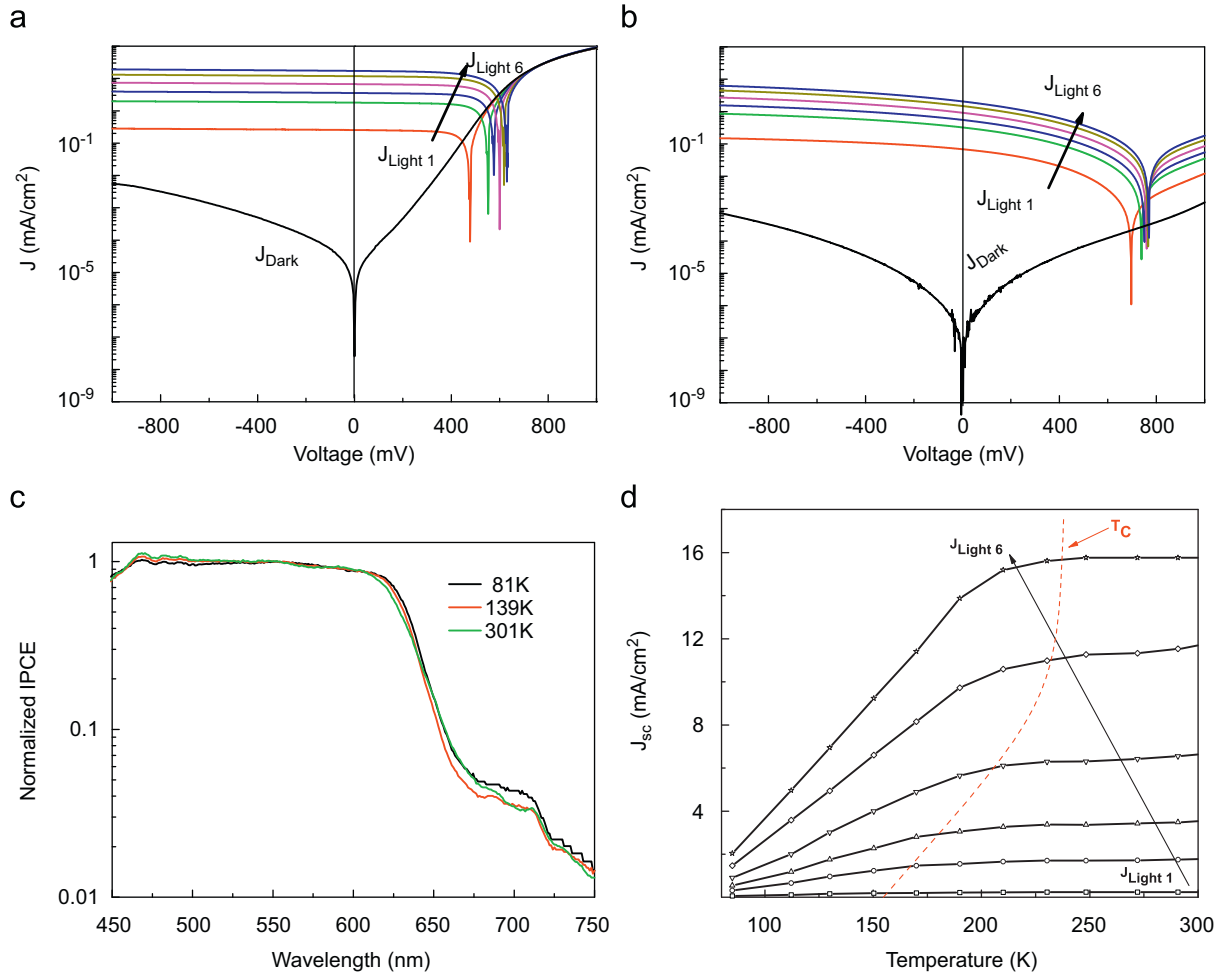


Fig. 3. J_{Light} and J_{Dark} versus applied voltage at (a) 300 K, (b) 85 K, (c) normalized IPCE spectra at different temperatures and (d) J_{SC} versus T at different intensities.

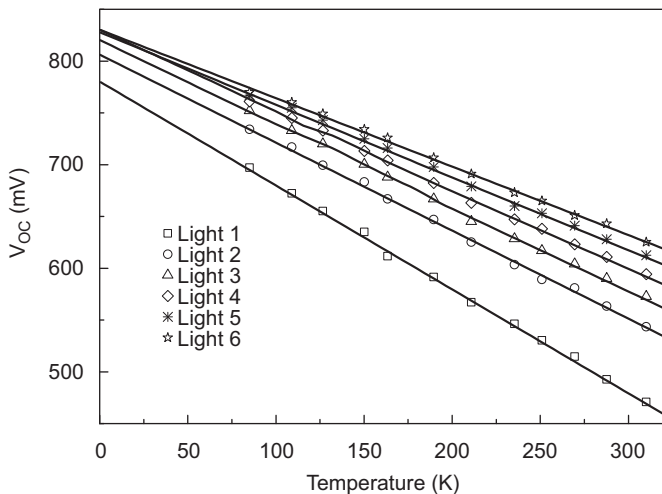


Fig. 4. Extrapolated plot of V_{OC} (mV) at different illumination intensity versus temperature (K). Values up to 85 K are experimentally obtained below those temperature curves that are extrapolated by using graphics software Origin 6.1.

This equilibrium is shifted toward high quasi Fermi levels splitting if G increases or R decreases, which has been shown in Fig. 4.

In Fig. 4, the V_{OC} at different intensities have been shown with respect to temperature. Measurements have been carried-out down to 85 K inside liquid nitrogen cryostat and curves have been extrapolated to 0 K. Characteristically similar results have

been obtained by Vandewal et al. [11]; the curves converge at 0 K and give maximum attainable V_{OC} . However, in our experiments, convergence only appears under high illumination intensities. The curves of V_{OC} versus temperature are still linearly dependent on temperature but they do not converge at 0 K under lower intensities of illumination. It has also been reported in literatures that maximum of V_{OC} is related to the band gap of the blend [17,18] but recombination mechanisms play a crucial role in the observable V_{OC} values [16].

Assuming Gaussian DOS of both the donor highest-occupied molecular orbital (HOMO) and the acceptor lowest-unoccupied molecular orbital (LUMO) manifolds, a straightforward calculation allows determining the Fermi level positions from which V_{OC} results proportional to the logarithmic function of the carrier density and E_g as [19]

$$qV_{OC} \propto E_g - k_B T \ln \left(\frac{N_n N_p}{n p} \right). \quad (1)$$

Here N_n (N_p) corresponds to the effective acceptor LUMO (donor HOMO) density-of-states, n (p) the electron (hole) concentration, and $k_B T$ stands for the thermal energy. It is important to emphasize that Eq. (1) is a high-temperature approximation, which may be extended to lower temperature regimes. Its application is valid if low-occupancy conditions are satisfied ($n \ll N_n$ and $p \ll N_p$). The temperature dependence of Eq. (1) might be rather complex. In addition to the explicit dependences on T , n and p vary with temperature. Charge carrier densities in the cell will be determined by the generation-recombination of kinetic

balance under constant illumination. In case of temperature-independent photo-generation, carrier density increases at lower temperatures because recombination is slowed down hence increasing V_{OC} . An exact interpretation of the open-circuit voltage dependence on temperature may be carried out by numerical simulation.

At constant temperature, open-circuit decay is governed by the electron-hole recombination processes. Calculating the time derivative of Eq. (1), one obtains the following expression:

$$q \frac{dV_{OC}}{dt} = k_B T \frac{d}{dt} \ln(np) = -k_B T \left(\frac{1}{\tau_n} + \frac{1}{\tau_p} \right), \quad (2)$$

where $(1/\tau_n) = -(1/n)(dn/dt)$ and $(1/\tau_p) = -(1/p)(dp/dt)$ allow defining the electron and hole lifetime, respectively. The lifetime measured by transient decay of V_{OC} is combination of both electron and hole lifetimes. An effective lifetime $\tau_{eff} = ((1/\tau_n) + (1/\tau_p))^{-1}$ results in accordance with the detailed model previously reported [20]; its physical interpretation is the charge carrier with shortest lifetime controlling the decay of V_{OC} as

$$\tau_{eff} = -\frac{k_B T}{q} \left(\frac{dV_{OC}}{dt} \right)^{-1}. \quad (3)$$

There are two limiting cases of application depending on the amount of photo-generated carriers in relation to the intrinsic or doping levels, i.e. n_0 , p_0 . We assume here a bimolecular recombination law $(dn/dt) = -\gamma np$ (here γ stands for the recombination coefficient) and electroneutrality conditions $n=p$. If $n > n_0$ and $p > p_0$, the lifetime results in being concentration-dependent as [20] $\tau_n = (1/\gamma n)$ what it entails is a reduction of lifetime for larger V_{OC} . The opposite situation occurs when $p \approx p_0$ (photo-generated holes do not exceed the doping level). In this last case, $\tau_{eff} = \tau_n$ strictly holds because there is no modulation of hole concentration. Electrons are now considered as minority carriers and then $\tau_n = (1/\gamma p_0)$ attains a constant value, independent of the V_{OC} . This implies a monomolecular-like decay law. By examining Fig. 5, we can observe two regimes for times longer than the resolution limit of the acquisition sampling system. At high temperatures (300 K) lifetime exhibits an almost constant value around 500 μs ($V_{OC} < 0.25$ V) that is reduced for higher V_{OC} . A more pronounced constant plateau is observed at intermediate temperatures (200 K) reaching higher open-circuit values ($V_{OC} < 0.4$ V). We interpret this behavior as resulting from the transition between monomolecular (low V_{OC}) to bimolecular (high V_{OC}) decay law.

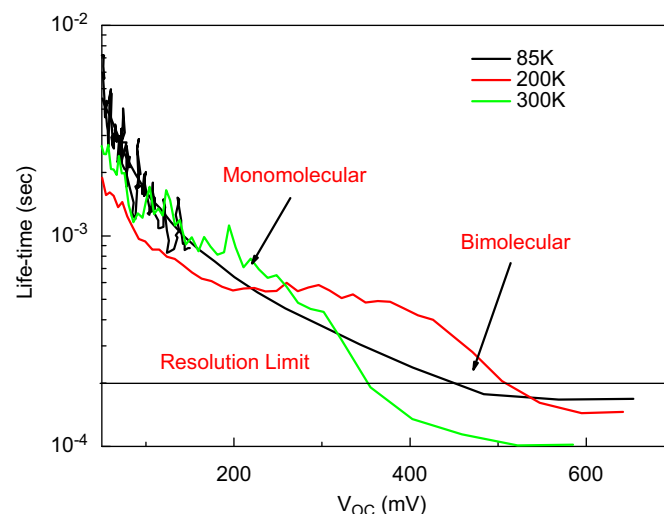


Fig. 5. Effective time constants (τ_{eff}) versus V_{OC} at different T calculated from Eq. (3). The V_{OC} decay has been measured at one illumination level by applying a square wave of frequency 1.25 Hz on LED as per the experimental set-up in Fig. 1.

Assuming typical doping levels $p_0 = 10^{16} \text{ cm}^{-3}$ and lifetime plateau values around 500 μs, we can estimate the recombination coefficient $\gamma = 1/\tau_n p_0$ which results in $2 \times 10^{-13} \text{ cm}^3 \text{ s}^{-1}$, in good agreement with values usually reported for this kind of solar cells [20–22]. At very low $V_{OC} < 0.1$ V recombination kinetics slows down as expected for deep trapping-mediated processes. The lifetime measurement at lower temperatures (85 K) has no simple interpretation. It is observed in Fig. 5 that the plateau of constant lifetime is not present. As shown in Fig. 3(d), current density only exhibits constant values at higher temperatures thus signaling the reduction of carrier extraction efficiency by the effect of decreasing mobility. The recombination mechanism will then also be limited by the transport of charge carriers at low temperatures. On the other hand, the lifetime plateau is related to the presence of ionized doping states. At very low temperatures the ionization of such impurities is no longer effective, which would imply a bimolecular recombination law at all temperatures.

4. Conclusions

In summary, from transient voltage decay, a transition from bimolecular to monomolecular recombination mechanisms for high and low V_{OC} has been observed, respectively, for the first time. This transition occurs at low V_{OC} at room temperature and is shifted towards high V_{OC} when T decreases. Under normal illumination conditions (AM1.5 100 mW/cm²) bimolecular recombination is the dominant mechanism. This should reflect why V_{OC} versus T curves get converged at 0 K only at high intensity whereas at low intensity V_{OC} is still linearly dependent on T but curves do not converge at 0 K.

Acknowledgements

This work has been supported by the French Research Agency (ANR) and the Region Aquitaine. G.G.B. and J.B. thank financial support from Ministerio de Educacion y Ciencia (Spain) under project HOPE CSD2007-00007 (Consolider-Ingenio 2010). We sincerely thank all our support staffs.

References

1. W. Shockley, J.H. Queisser, Detailed balance limit of efficiency of p-n junction solar cells, *J. Appl. Phys.* 32 (1961) 510–519.
2. S.H. Park, A. Roy, S. Beaupr, S. Cho, N. Coates, J.S. Moon, D. Moses, M. Leclerc, K. Lee, A.J. Heeger, Bulk heterojunction solar cells with internal quantum efficiency approaching 100%, *Nat. Photon.* 3 (2009) 297–302.
3. M.C. Scharber, D. Mühlbacher, M. Koppe, P. Denk, C. Waldauf, A.J. Heeger, C.J. Brabec, Design rules for donors in bulk-heterojunction solar cells—towards 10% energy-conversion efficiency, *Adv. Mater.* 18 (2006) 789–794.
4. M. Knupfer, Exciton binding energies in organic semiconductors, *Appl. Phys. A* 77 (2003) 623–626.
5. C.W. Tang, Two-layer organic photovoltaic cell, *Appl. Phys. Lett.* 48 (1986) 183–185.
6. D. Chirvase, Z. Chiguvare, M. Knipper, J. Parisi, V. Dyakonov, J.C. Hummelen, Temperature dependent characteristics of poly(3 hexylthiophene)-fullerene based heterojunction organic solar cells, *J. Appl. Phys.* 93 (2003) 3376–3383.
7. I. Riedel, V. Dyakonov, Influence of electronic transport properties of polymer-fullerene blends on the performance of bulk heterojunction photovoltaic devices, *Phys. Stat. Sol. (a)* 201 (2004) 1332–1341.
8. V. Dyakonov, Mechanisms controlling the efficiency of polymer solar cells, *Appl. Phys. A* 79 (2004) 21–25.
9. I. Riedel, E.V. Hauff, J. Parisi, N. Martin, F. Giacalone, V. Dyakonov, Diphenylmethanofullerenes: new and efficient acceptor in bulk-heterojunction solar cells, *Adv. Funct. Mater.* 15 (2005) 1979–1987.
10. P.B. Rand, P.D. Burk, S.R. Forrest, Offset energies at organic semiconductor heterojunctions and their influence on the open-circuit voltage of thin-film solar cells, *Phys. Rev. B* 75 (2007) 115327.
11. K. Vandewal, K. Tvingstedt, A. Gadisa, O. Inganäs, J.V. Manca, Relating the open-circuit voltage to interface molecular properties of donor:acceptor bulk heterojunction solar cells, *Phys. Rev. B* 81 (2010) 125204.

- [12] L.J.A. Koster, V.D. Mihailescu, R. Ramaker, P.W.M. Blom, Light intensity dependence of open-circuit voltage of polymer:fullerene solar cells, *Appl. Phys. Lett.* 86 (2005) 123509.
- [13] T. Tromholt, E.A. Katz, B. Hirsch, A. Vossier, F.C. Krebs, Effects of concentrated sunlight on organic photovoltaics, *Appl. Phys. Lett.* 96 (2010) 073501-073503.
- [14] J. Bisquert, D. Cahen, G. Hodes, S. Rühle, A. Zaban, Physical chemical principles of photovoltaic conversion with nanoparticulate, mesoporous dye-sensitized solar cells, *J. Phys. Chem. B* 10 (8) (2004) 8106–8118.
- [15] M. Riede, T. Mueller, R. WTress, K. Schueppelnd, Leo, small-molecule solar cells—status and perspectives, *Nanotechnology* 19 (2008) 424001.
- [16] Germà Garcia-Belmonte, Juan Bisquert, Open-circuit voltage limit caused by recombination through tail states in bulk heterojunction polymer–fullerene solar cells, *Appl. Phys. Lett.* 96 (2010) 113301.
- [17] L.J.A. Koster, V.D. Mihailescu, P.W.M. Blom, Ultimate efficiency of polymer/fullerene bulk heterojunction solar cells, *Appl. Phys. Lett.* 88 (2006) 093511.
- [18] G. Dennler, M.C. Scharber, C.J. Brabec, Polymer–fullerene bulk-heterojunction solar cells, *Adv. Mater.* 21 (2009) 1323–1338.
- [19] Germà Garcia-Belmonte, Temperature dependence of open-circuit voltage in organic solar cells from generation-recombination kinetic balance, *Sol. Energy Mater. Sol. Cells* 94 (2010) 2166–2169.
- [20] Germà Garcia-Belmonte, P.P. Boix, J. Bisquert, M. Sessolo, H.J. Bolink, Simultaneous determination of carrier lifetime and electron density-of-states in P3HT:PCBM organic solar cells under illumination by impedance spectroscopy, *Sol. Energy Mater. Sol. Cells* 94 (2010) 366–375.
- [21] A. Foertig, A. Baumann, D. Rauh, V. Dyakonov, C. Deibel, Charge carrier concentration and temperature dependent recombination in polymer–fullerene solar cells, *Appl. Phys. Lett.* 95 (2009) 052104.
- [22] R. Hamilton, C.G. Shuttle, B. O'Regan, T. Hammant, J. Nelson, J.R. Durrant, Recombination in annealed and non annealed polythiophene/fullerene solar cells: transient photovoltage studies versus numerical modelling, *J. Phys. Chem. Lett.* 1 (2010) 1432–1436.